Desalination and Water Treatment
www.deswater.com

doi:10.5004/dwt.2018.22107

107 (2018) 72–84
March

Activated carbon embedded chitosan/polyvinyl alcohol biocomposites for adsorption of nonsteroidal anti-inflammatory drug-naproxen from wastewater

Didem Saloglu*, Nazli Ozcan

Yalova University, Engineering Faculty, Department of Chemical and Process Engineering, 77100, Yalova, Turkey
Tel. +90-2268155392, email: didemsalogludertli@gmail.com (D. Saloglu), nazliozcan_kmy@windowslive.com (N. Ozcan)

Received 11 November 2017; Accepted 24 February 2018

ABSTRACT

The feasibility of using activated carbon/chitosan-poly (vinyl alcohol) biocomposites (AC/CHT-PVA) as an adsorbent for removal of naproxen from a factory wastewater in Tuzla, Istanbul/Turkey was studied in the presented study. The biocomposites were synthesized with different AC: CHT-PVA ratios of 1.0; 2.0 and 3.0 (w/w). The adsorbent materials were characterized by FT-IR, SEM and TGA analysis. When AC was embedded into CHT-PVA matrix, the naproxen removal performance increased from 41.01% to 97.03%. The optimal pH for maximum adsorption was found as 7.0. Equilibrium isotherms for the naproxen adsorption onto AC/CHT-PVA biocomposite were measured experimentally. The Langmuir model was fitted to the equilibrium data better than The Freundlich, Temkin and Dubinin-Raduskevich isotherm models. The mono layer adsorption capacity of AC/CHT-PVA:3.0 for naproxen was found to be 12.24 mg/g at 298 K. According to the kinetics results, the equilibrium time of AC/CHT-PVA biocomposites was found 100 min and it was indicated that the adsorption follows the pseudo second-order kinetic model. The process was favorable and spontaneous. The thermodynamic parameters, ΔG°, ΔS° and ΔH° were calculated and the enthalpy of adsorption (ΔH°) was found positive for all biocomposites supported the endothermic nature of adsorption reactions.

Keywords: Activated carbon; Adsorption; Chitosan; Composite; Kinetics; Naproxen

1. Introduction

Pharmaceutical compounds have recently been detected in sewage effluents, surface and ground water, domestic water and drinking water [1–3]. Pharmaceuticals perform as a obstacle for some chemicals and oxidizing agents because of their molecular structure [4]. Drug active substances at ppm levels have the potential to cause negative effects for human and removal of these compounds through drinking and domestic water treatment processes is therefore emerging concern [5,6].

Naproxen (2-naphthaleneacetic acid, 6-methoxy-a-methyl-,(S)-(+)-(S)-6-methoxy-alpha-methyl-2-naphthaleneacetic acid) belongs to propionic acid derivatives, is a non-steroidal anti-inflammatory drug and treats for fever and reducing pain [7,8]. Naproxen exists in the range of 0.1–2.6 μg/L in plant effluents waste water and in the range of 0.01–0.1 μg/L in surface water [9–11]. The conventional separation processes has been shown to be an ineffective method in the removal of trace amount of pharmaceutical products such as naproxen, bisphenol A etc. [12–17].

It is proposed that, adsorption would be promising for the separation of micro pollutants from waste water. The suitable adsorbent selecting increases the water treatment efficiency. Carbon based adsorbents are effective for removing micro pollutants such as pharmaceutical compounds. Carbon based materials such as activated carbon, carbon nanotubes etc. have been of interest due to high surface area and pore size distribution. Also, in the past decade,

*Corresponding author.

carbon containing polymeric composites with high adsorption capacity, high adsorption rate are the precursors in the searching for new adsorbents [18,19].

Chitosan is composed of partially deacetylate material of chitin, having amine groups [20]. Because it contains a large number of amine groups, chitosan and its derivatives have been widely applied as a biocomposite, especially in adsorption technology [21,22]. Several materials have been used to synthesize the composites with chitosan, such as carbon derivatives, silver nano particles, sand, perlite, clay, spirulina, poly (vinyl alcohol), and poly (vinyl chloride), and acrylamide [23–29].

This research work analyzed the synergistic effects of chitosan, poly (vinyl alcohol) and activated carbon on pharmaceutical compounds removal from waste waster. The objective and the originality of the present paper are, to test adsorption behavior of activated carbon embedded chitosan-poly (vinyl alcohol) biocomposites (AC/CHT-PVA) for the removal of naproxen from wastewater collected from a drug factory in Tuzla, Istanbul/Turkey. The morphological and chemical properties of biocomposites were characterized by FT-IR, SEM and TGA analysis. The behavior of the adsorption was considered on the effect of pH, temperature, adsorbent dosage and time. The Langmuir, Freundlich, Temkin and D-R adsorption isotherms and pseudo-first order, pseudo-second order, Elovich, Weber–Morris and Bangham kinetics models were also studied. The thermodynamic parameters were also evaluated from the adsorption measurements and $\Delta G°$, $\Delta S°$ and $\Delta H°$ were calculated. It can be safely stated that, this work represents the first in the literature to follow the adsorption behavior of AC/CHT-PVA biocomposites for the removal of naproxen.

2. Materials and methods

2.1. Preparation of CHT-PVA matrix

Firstly, chitosan was dispersed in 2% aqueous solution of acetic acid and stirred for 12 h until complete dissolution and obtain a 5% (w/v) solution. 1 g of PVA was dissolved in 50 mL of hot water and stirred for 24 h at 80°C to allow dissolution. A mixture of 30 mL CHT solution and 30 mL PVA solution was stirred overnight at 60°C to form a homogeneous solution with volumetric CHT:PVA (v/v) ratio of 1.0. Then, glutaraldehyde (1%, w/w) was drop wise added to CHT-PVA solution and kept under stirring for 24 h. CHT-PVA was washed with distilled water for removal of unreacted compounds, dried at room temperature and further dried in freeze-dryer.

2.2. Preparation of AC/CHT-PVA biocomposites

AC/CHT-PVA biocomposites were synthesized with different AC:CHT-PVA ratios of 1.0–3.0 (w/w). AC with defined weight fractions were added into CHT-PVA solution and the mixtures were dispersed until complete dissolution and obtain a homogenous mixture. Then, glutaraldehyde solution was dropwise added to the AC/CHT-PVA mixtures. After cross linking reaction, biocomposites were washed and dried as described above. The biocomposites were coded as AC/CHT-PVA:(1.0–3.0). The schematic reaction mechanism is represented in Fig. 1.

2.3. Determination of naproxen

Naproxen concentrations were analyzed using UV-vis spectrophotometer (Shimadzu UV1800) at 230 nm wavelength in water using 1 cm quartz match cells. For dilutions various micro pipettes of volumes 10–100 µl were used [30].

Each experiment was duplicated under identical conditions and average results were reported.

2.4. Characterization of biocomposites

N_2 adsorption measurements were performed using a Micro meritics ASAP 2020 surface analyzer. The specific surface area and pore volumes were obtained from nitrogen adsorption data at 77 K and surface areas were calculated by the Branauer–Emmett–Teller (BET) method. The molecular structure of the CHT-PVA and AC/CHT-PVA was defined by a Shimadzu, IR Affinity Spectrometer. The spectra were recorded by 16 scans with a resolution of 2 cm^{-1}. The surface morphology of was investigated by Scanning Electron Microscopy (Philips XL-30) and thermal characterization of the biocomposites was carried out by thermogravimetric analysis by Perkin Elmer, Diamond DSC (from 20°C to 800°C at 10°C/min heating rate).

2.5. Experimental procedures

To explain the adsorption mechanism of naproxen from factory wastewater onto AC/CHT-PVA biocomposites, the point of zero charges (pHzpc) were estimated. pHzpc of CHT-PVA and AC/CHT-PVA were measured using the pH drift method.

In batch adsorption experiment, 25 mL of 50 mg/L naproxen solution from factory wastewater was added to 20–200 mg of AC/CHT-PVA biocomposites in a 250 mL Erlenmeyer at 25 ± 0.5°C and adsorption experiment were performed on a mechanical shaker at 140 rpm. Then the biocomposites were separated from solution and absorbance values of the supernatants were measured at 230 nm to determine the residual naproxen concentrations after adsorption. Adsorption experiments were repeated three times under identical conditions, and the standard deviation was within ca. ±5%, also all results are reproducible.

Eq. (1) is used to calculate the adsorption capacity of naproxen:

$$q_e = \frac{(C_i - C_e) \times V}{m} \quad (1)$$

where q_e is adsorption capacity (mg/g), V is volume (L), m is amount of biocomposite (adsorbent, g), C_i and C_e are initial and equilibrium concentrations (mg/L), respectively.

The naproxen removal percentage (NR%) can be calculated from Eq. (2):

$$NR\% = \frac{(C_0 - C_e)}{C_0} \times 100 \quad (2)$$

The effects of initial naproxen concentration and amount of biocomposites on the adsorption kinetics were investigated. In order to determine the effect of pH values, batch adsorption experiments were done in the pH range

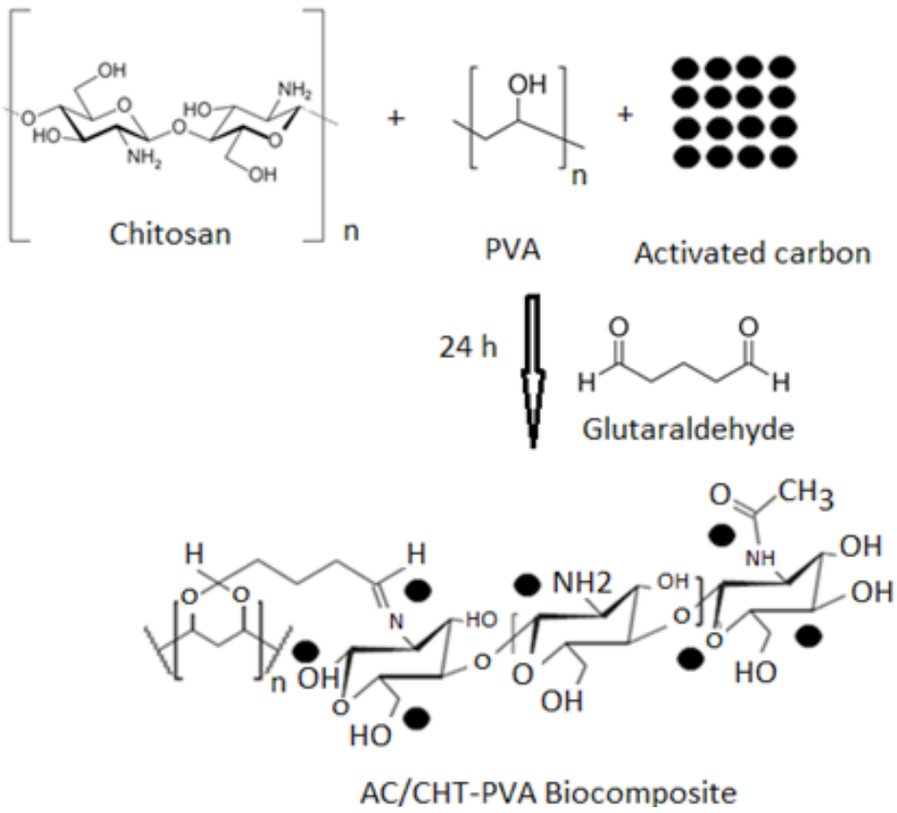

Fig. 1. Schematic representation of AC/CHT-PVA biocomposites synthesis mechanism.

from 3.0 to 11.0. The pH of naproxen solution from factory wastewater was adjusted by using NaOH or HCl solution during adsorption. Also, the effect of amount of adsorbent was detected by using 20–200 mg of biocomposite. The adsorption experiments were carried out at 25°C, 40°C, and 55°C and effect of temperature was investigated and thermodynamic parameters were calculated.

The kinetic experiments were carried out using 50 mg/L naproxen solution from factory wastewater with defined amount of biocomposites and the adsorption kinetics were investigated by pseudo-first order, pseudo-second order, Elovich, Weber–Morris and Bangham models [31,32].

Table 1
Physical properties of CHT, CHT-PVA, AC and AC/CHT-PVA:3.0

	Total pore volume (cm^3/g)	BET Surface area (m^2/g)
AC	0.736	687
CHT	<0.0001	4.58
CHT-PVA	0.0089	65.86
AC/ CHT-PVA:3.0	0.0027	198.28

3. Results and discussion

3.1. Characterization of biocomposites

Table 1 represents the effect of AC on the BET surface area and pore volume of AC/CHT-PVA biocomposite. The BET surface areas for the AC, CHT, CHT-PVA, and AC/CHT-PVA:3.0 samples were 687 m^2/g, 4.58 m^2/g, 65.86 m^2/g and 198.28 m^2/g, respectively. CHT is observed to have the least specific surface area while AC has the highest surface area and the biocomposites resulted in a larger surface area than that of chitosan but less than that of AC. The BET surface area is in the order of AC>AC:CHT-PVA:3.0>CHT-PVA>CHT. The lower BET surface area and pore volume of AC/CHT-PVA was due to chitosan molecules blocking the pores of activated carbon. Also it can be safely stated that, the improvement of the chitosan properties may occur because AC acts as a support for it.

FT-IR analysis is employed to detect the interaction between CHT, PVA and AC. Fig. 2 demonstrates the FT-IR spectra for all biocomposites before adsorption process. As shown in the figure, the broad band with a maximum force near 3280 cm^{-1} induces the valance vibration of binding –OH on -N-H intensely involved in hydrogen bindings and the band at 2880 cm^{-1} is identified by –C-H bond. The characteristic peak at 1650 cm^{-1} associates with the imine C=N bond form by the reaction of amino group of chitosan and aldehyde groups from glutaraldehyde as a cross linking

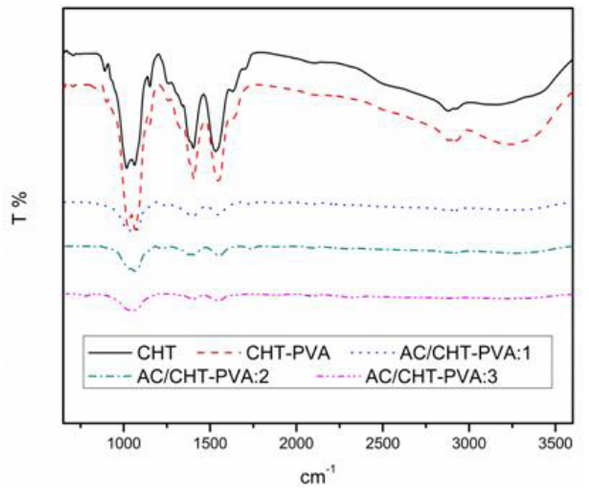

Fig. 2. FT-IR spectra of CHT, CHT-PVA and AC/CHT-PVA biocomposites.

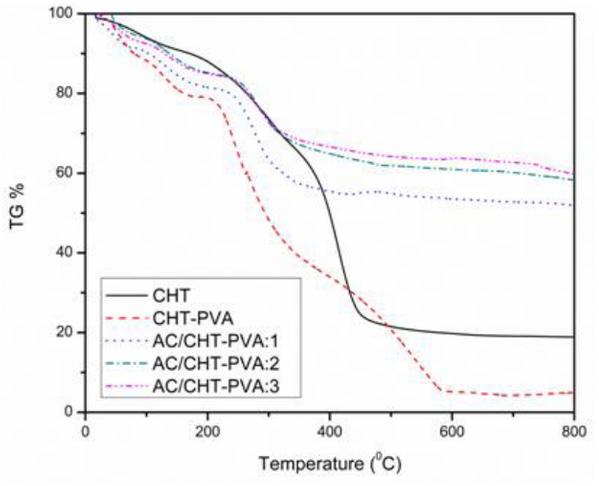

Fig. 3. TGA curves of CHT, CHT-PVA and AC/CHT-PVA biocomposites.

agent, can be identified. The adsorption peak at 1080 cm^{-1} indicates –N-H stretching vibration. Several spectacular differences appeared in the FT-IR spectra of AC/CHT-PVA biocomposites in comparison with the others. The band at 3280 cm^{-1} did not occur for all AC/CHT-PVA biocomposites. The bands near 3280 cm^{-1} and 2880 cm^{-1} are weaken extremely showing that AC substantially bonded with the -OH, -C–H and -N–H groups of CHT-PVA matrix.

The thermal stabilities of biocomposites are confirmed by TGA. Fig. 3 exhibits the TGA thermograms of AC/CHT-PVA biocomposites as well as CHT and derivative curves of biocomposites' weight losses. From TGA trace, in temperature range of 25°C to 800°C, the biocomposites degraded at a faster rate than AC. The char yield of all the AC/CHT-PVA biocomposites was found to be intensely higher than that of CHT and CHT-PVA. The char yield ratio increased with increasing AC ratio. AC had only 70% of total loss nearly 400°C (data not shown). After the embedding the AC, the char yield values reached almost 30–35% at higher temperatures, resulting from the degradation of intercalated and edge attached AC. CHT-PVA decomposed (70%) between 50°C and 400°C compared to AC/CHT-PVA:3.0 and AC/CHT-PVA:2.0 (35% and 40%) due to the higher AC content. The char yield ratios were found as 5%; 50%; 60% and 65% for CHT-PVA; AC/CHT- PVA:1.0; AC/CHT-PVA:2.0 and AC/CHT-PVA: 3.0, respectively. The highest residue and the lowest degradation rate were accomplished for AC/CHT-PVA:3.0.

SEM images at low and high magnifications in Figs. 4 and 5 illustrate surface morphologies of both CHT-PVA and biocomposites. It is obvious that, CHT-PVA possessed the large open cells with sizes in ca 200–250 micrometer containing 20 micrometer sized small open co-pores. This morphology made CHT-PVA more attractive for activated carbon accommodation. It can be apparently seen from the figure that, surface morphology of CHT-PVA was changed distinctively with introducing AC. With increasing AC content, pore sizes decreased from 30 micrometer to nearly 0.5 micrometer. AC/CHT-PVA:1.0 and AC/CHT-PVA:2.0 are coated by non-uniform pores with sizes ranging from 5–30 micrometer. The existence of a similar polymeric surface has been described for both biocomposites, and is obviously interested to decorating of surface pores by adding AC to CHT-PVA's large pores.

A totally different structure was found for AC/CHT-PVA:3.0. The biocomposite exhibited a close and homogeneous network structure, with small pores sized ranging from ca 0.5 µm upon 10 µm. In AC/CHT-PVA:1.0 and AC/CHT-PVA:2.0, their interior structures were more irregular than the ones found in AC/CHT-PVA:3.0.

According to the high magnification SEM images, AC/CHT-PVA:3.0 has a sub-porous structure (Fig. 5). The biocomposite did not exhibit a porous structure in weak magnitude SEM image, but very small pores and tubular morphology with 0.5 µm occurred in higher magnification of the SEM images. On the other hand, as illustrated in the figure, when focused on the AC/CHT-PCA:3.0 surface area, more regular small rooms and pores, pores in pores at the rod ends, and spaces in between were obviously different compared to the others' surface. After AC embedding process, there was a significant increase in micro fractures. Fractures covering the entire surface and providing a uniform area were believed to be the result of the formation of sub-networks.

3.2. Adsorption of naproxen from a factory wastewater onto biocomposites

The results for the naproxen removing from factory wastewater using different of AC/CHT-PVA (20–200 mg/25 ml) are demonstrated in Fig. 6. The adsorption capacity decreased with increasing amount of biocomposites. This situation indicated that, the adsorption capacities refined consequently (nearly 3.5 times higher) when activated carbon embedded into the CHT-PVA. As the AC ratio increases from 0.0 to 3.0 for 50 mg of adsorbent at pH 7.0, adsorption capacity and removal percentage increased from 4.82 mg/g to 16.86 mg/g and from 22.0% to 67.01%, respectively.

Also Fig. 7 displays the removal (%) values of CHT-PVA and AC/CHT-PVA biocomposites. The naproxen adsorption capacity values were determined as 6.75 mg/g; 9.65 mg/g; 10.80 mg/g and 12.17 mg/g for CHT-PVA; AC/

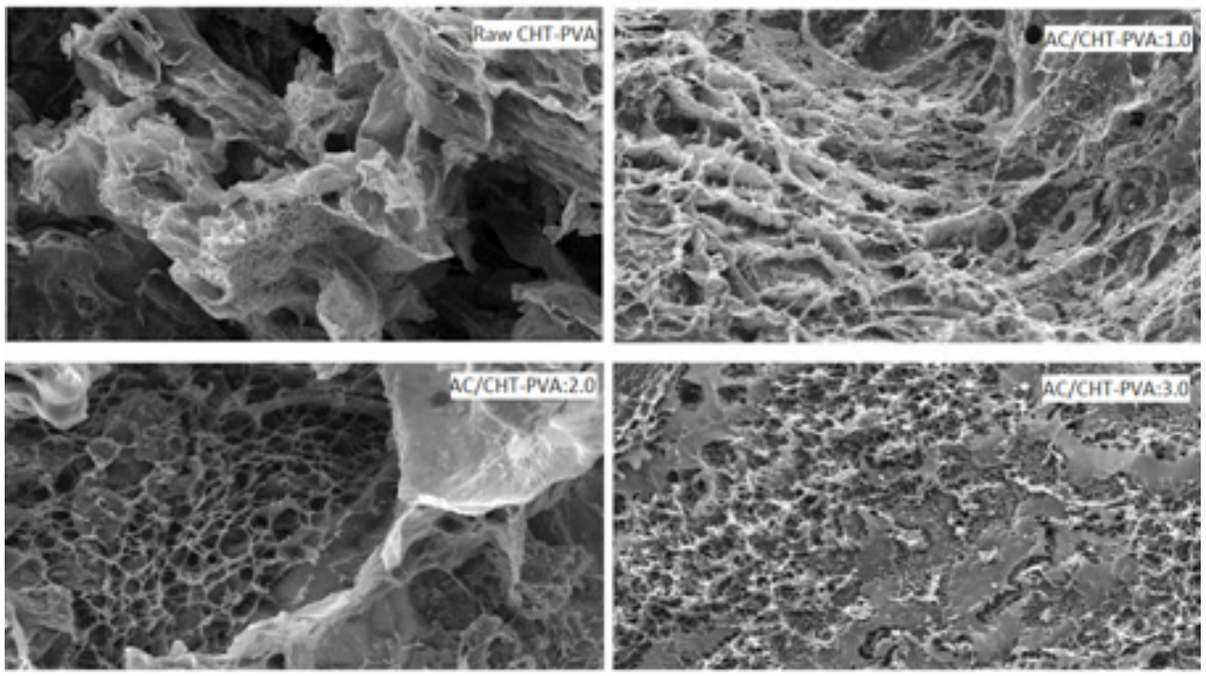

Fig. 4. SEM images of surface region (a) CHT-PVA (×1000); (b) AC-CHT-PVA:1.0 (×1000); (c) AC/CHT-PVA:2.0 (×1000), and (d) AC/CHT-PVA:3.0 (×1000).

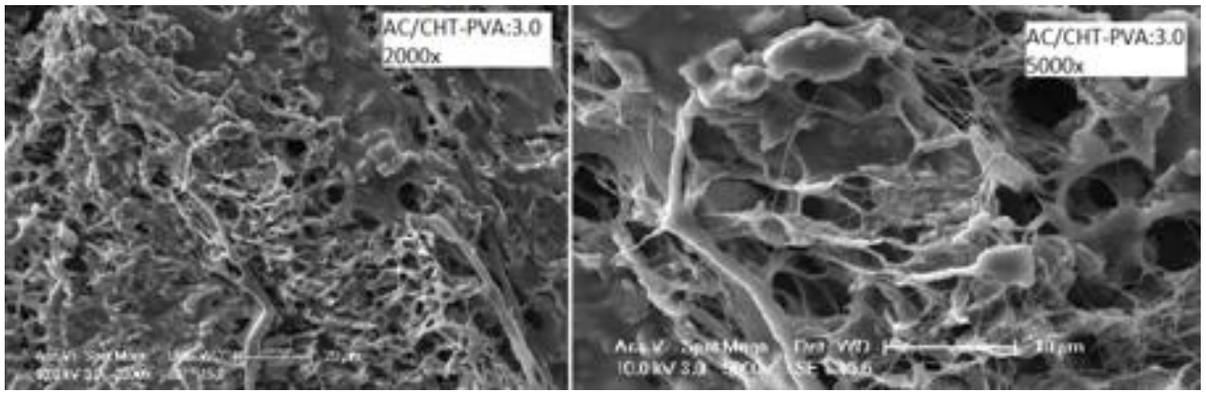

Fig. 5. High magnification SEM images of AC/CHT-PVA:3.0 (×2000) and (×5000).

CHT-PVA:1.0–3.0. Removal (%) values of adsorption were detected as 54.30%; 77.21%; 84.44% and 97.36% using 100 mg of CHT-PVA and AC/CHT-PVA:1.0; AC/CHT-PVA:2.0 and AC/CHT-PVA:3.0, respectively.

It can be concluded that, amount of AC increases from 0.0 to 3.0, adsorption removal (%) values raised seriously from 54.30% to 97.36% (Fig. 7). Thus, 100 mg of AC/CHT-PVA:3.0 was preferred as the optimum amount of biocomposite for the further experiments.

The effect of pH on the adsorption of naproxen from factory wastewater is demonstrated in Fig. 8. The results indicated that q_e values (for AC/CHT-PVA:3.0) boosted from 9.74 mg/g to 12.24 mg/g with rising pH from 3.0 to 7.0. pH value of the naproxen changed further, the naproxen adsorption capacity was not changed effectively.

CHT-PVA (pH_{ZP} = 4.5) is positively charged at pH values are between 3.0 and 4.0 and it cannot absorb –N-H of naproxen. When pH is above 6.2, the surface of the AC/CHT-PVA (pH_{ZPC} = 6.2) becomes negatively charged, which begins to adsorption cations belongs to naproxen through the electrostatic force of attraction. The maximum adsorption rates were obtained at neutral and above neutral pH values as the progress of negative charge surface of the AC/CHT-PVA.

The removal behavior of naproxen from factory wastewater was lower at acidic pHs than neutral and basic pH values. q_e value for AC/CHT-PVA/CF:1.0 increased from 6.85 mg/g at pH 3.0 to 10.13 mg/g at pH 11.0 while that increased from 9.74 mg/g at pH 3.0 to 12.40 mg/g at pH 11.0 for AC/CHT-PVA:3.0. At basic pH values, positively

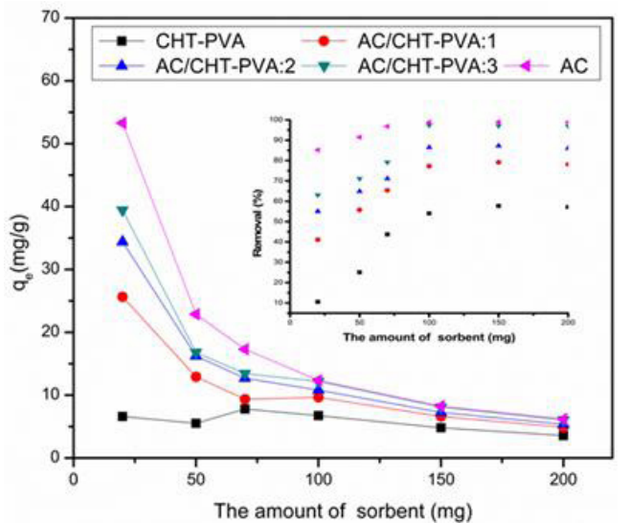

Fig. 6. Effect of adsorbent dosage on the naproxen adsorption.

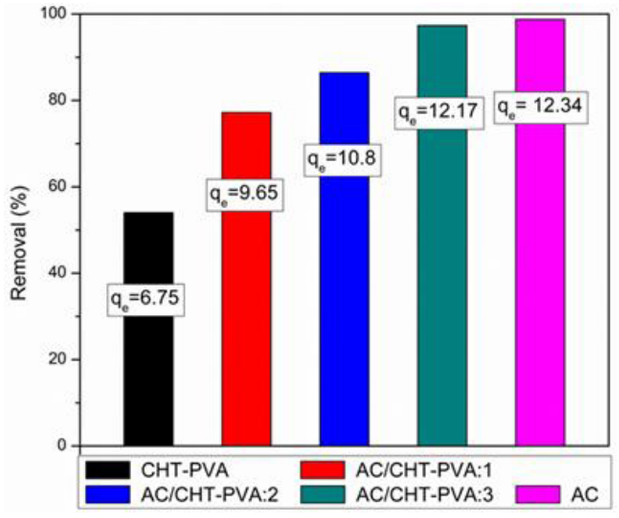

Fig. 7. Naproxen removal percentages of CHT-PVA and AC/CHT-PVA biocomposites at 100 mg adsorbent dosage.

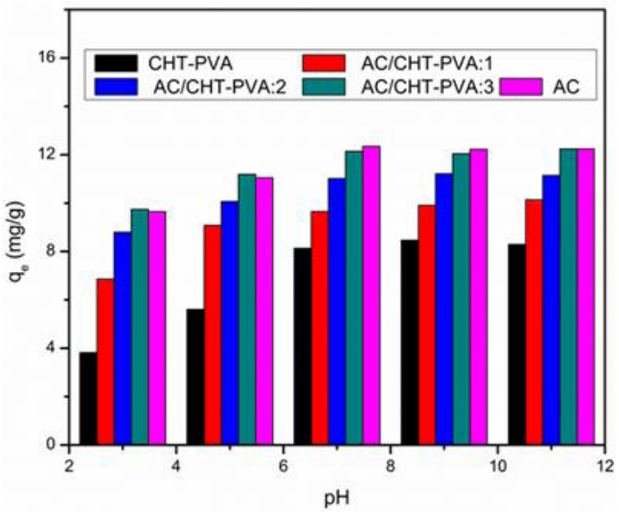

Fig. 8. Effect of pH on the naproxen adsorption.

Table 2
Adsorption isotherm model equations

Langmuir isotherm model	$q_e = \frac{Q \cdot b}{1 + b \cdot C_e}$
	$R_L = \frac{1}{1 + b \cdot C_0}$
Freundlich isotherm model	$q_e = K_F \cdot C_e^{1/n}$
Temkin isotherm model	$q_e = \frac{RT \ln(A_t \cdot C_e)}{B}$
Dubinin-Radushkevich (D-R) isotherm model	$q_e = Q \exp(-\beta \cdot \varepsilon^2)$
	$\varepsilon = R \cdot T \ln(1 + \frac{1}{C_e})$
	$E = \frac{1}{\sqrt{2\beta}}$

charged naproxen cations can be adsorbed on the negatively charged biocomposite surface. q_e values reached maximum values of 10.13 mg/g; 11.14 mg/g; 12.24 mg/g at pH 11.0 for AC/CHT-PVA:1.0, AC/CHT-PVA:2.0, and AC/CHT-PVA:3.0, respectively. The naproxen adsorption on activated carbon (pH_{ZPC} = 7.1) displayed related tendency with AC/CHT-PVA biocomposites. q_e value lightly expanded from 9,69 mg/g at pH 3.0 to 12.26 mg/g at pH 7.0 and 11.0. Consequently, pH 7.0 was chosen as optimum pH for further experiments.

3.3. Adsorption isotherms of naproxen from a factory wastewater

The relationship between the naproxen adsorption and the equilibrium concentrations are characterized by Langmuir, Freundlich, Temkin and Dubinin–Radushkevich (D-R) models (Table 2). Table 3 and Fig. 9 illustrate the related model parameters.

Fig 9 demonstrates these adsorption isotherms of all biocomposites and activated carbon by linear analysis. Langmuir, Freundlich, Temkin and D-R model parameters and correlation coefficients (R^2) are presented in Table 3.

According to the R^2 values each model in Table 3, the Langmuir model fitted the best, although Temkin and D-R fitted worst. The linear regression coefficient (R^2) values changed between 0.84 and 0.98 and the isotherm can be approved fitting the Langmuir equation well. Q and b values were calculated from the linearization to be 1.949 mg/g and 0.2305 L/mg for CHT-PVA, and 31.152 mg/g and 0.4639 L/mg for AC/CHT-PVA:3.0, respectively. R_L

Table 3
Adsorption isotherm model parameters of the naproxen adsorption

	CHT-PVA	AC/ CHT-PVA:1.0	AC/ CHT-PVA:2.0	AC/ CHT-PVA:3.0	AC
Langmuir isotherm model					
Q (mg/g)	1.949	71.151	47.610	31.152	42.190
b	0.2305	0.0129	0.0703	0.4639	0.6287
R_L	0.079	0.607	0.222	0.041	0.030
R^2	0.97	0.98	0.98	0.84	0.89
Freundlich isotherm model					
K_F (mg/g)	0.592	0.971	0.608	0.430	0.560
$1/n$	1.053	0.127	4.685	9.883	14.679
R^2	0.90	0.85	0.92	0.92	0.93
Temkin isotherm model					
A_t (L/mg)	0.1644	0.1313	0.3972	1.9611	2.6960
B (kJ/mol)	5.015	15.016	14.139	9.541	14.977
R^2	0.87	0.76	0.84	0.82	0.81
Dubinin-Radushkevich (D-R) isotherm model					
Q (mol/g)	11.22	21.74	29.74	27.21	34.47
β	5E–05	2E–05	6E–06	4E–07	2E–07
E (kJ/mol)	0.100	0.158	0.288	1.118	1.581
R^2	0.85	0.64	0.73	0.62	0.66

values were determined as 0.079; 0.607; 0.222; 0.041 and 0.030 for CHT-PVA, AC/CHT-PVA:1.0, AC/CHT-PVA:2.0, AC/CHT-PVA:3.0 and AC, respectively (Fig. 9a). These calculated results indicate that naproxen adsorption on AC/CHT-PVA follow the Langmuir monolayer adsorption.

Based on the correlation of q_e versus C_e, the Freundlich model is demonstrated in Fig. 9b. The Freundlich model constants were calculated and exhibited in Table 3. K_F and $1/n$ parameters were calculated to be 0.592 L/g and 1.053 for CHT-PVA, and 0.430 and 9.883 for AC/CHT-PVA:3.0, respectively. As the value of $1/n$ is lower than 1.0, it is point out a favorable adsorption. For the naproxen adsorption, all $1/n$ values are higher than 1.0, so Freundlich model is not favorable for the naproxen adsorption.

It can be displayed in Table 3 and Fig. 9c, for Temkin model R^2 values were positioned within 0.76–0.87, which refer roughly fit to the naproxen adsorption. Also, Table 3 shows that, heat of the naproxen adsorption was restricted within 5.015 kJ/mol–15.016 kJ/mol. B (heat constant for Temkin) values were estimated as 9.571 kJ/mol; 5.015 kJ/mol and 14.977 kJ/mol for AC/CHT-PVA:3.0; CHT-PVA and AC, respectively. Temkin adsorption potential of naproxen, A_t values were calculated as 1.9611 L/mg for AC/CHT-PVA:3.0 and 2.6960 L/mg for AC. According to adsorption isoterm model parameters results (Table 3 & Fig. 9d), the mean free energy values of adsorption calculated from D-R model, were in the range of 0.100 kJ/mol–1.581 kJ/mol. The mean free energy values were found in the range of 0.100 kJ/mol and 0.288 kJ/mol for CHT-PVA and AC/CHT-PVA:2.0, respectively; while that of for AC and AC/CHT-PVA:3.0 were determined as 1.581 kJ/mol and 1.118 kJ/mol, respectively.

When mean free energy is below 8 kJ/mol, adsorption is approved as physical adsorption. In contrast, if this value is restricted between 8 kJ/mol and 16 kJ/mol, process is accepted as chemical adsorption. It can be detected from Table 3, calculated mean free energy values from linear regression, and are limited within the range of 0.100 kJ/mol and 1.581 kJ/mol. According to the results, we concluded that, the naproxen adsorption seemed to be a mono layer and physical sorption and the adsorption takes place on a non-uniform surface.

3.4. Kinetic studies of adsorption of naproxen from a factory wastewater

Effect of time of the adsorption from factory wastewater are exhibited in Figs. 10 a,b. The naproxen adsorption on CHT-PVA was very fast during the first 1 h, then continued at a slower adsorption rate and reached equilibrium at the end of 1.5 h and Ce value was estimated as 20 mg/L after 1.5 h. Also, in adsorption processes with AC, AC/CHT-PVA:2.0 and AC/CHT-PVA:3.0 reached equilibrium at the end of 4 h and Ce values were determined as nearly 2,17 mg/L, 3,69 mg/L and 5,58 mg/L, and q_e values were measured as 11.0 mg/g and 12.34 for AC; AC/CHT-PVA:2.0 and AC/CHT-PVA:3.0, respectively, until end of the experiment.

Various kinetics models have been proposed to define the adsorption mechanism. Pseudo-first-order, pseudo-second-order, Elovich, Weber–Morris intra-particle diffusion, and Bangham models were applied the naproxen adsorption in the present study (Table 4). ln $(q_e - q_t)$ and t/q_t vs. time (min) for pseudo 1st and 2nd order reaction kinetics are shown in Figs. 11a,b. k_1 (min^{-1}) and k_2 (g/mg·min) are the rate constant of the models, and $h = k_2 q_e^2$ where h is initial adsorption rate (mg/g·min) for 2nd order reaction model.

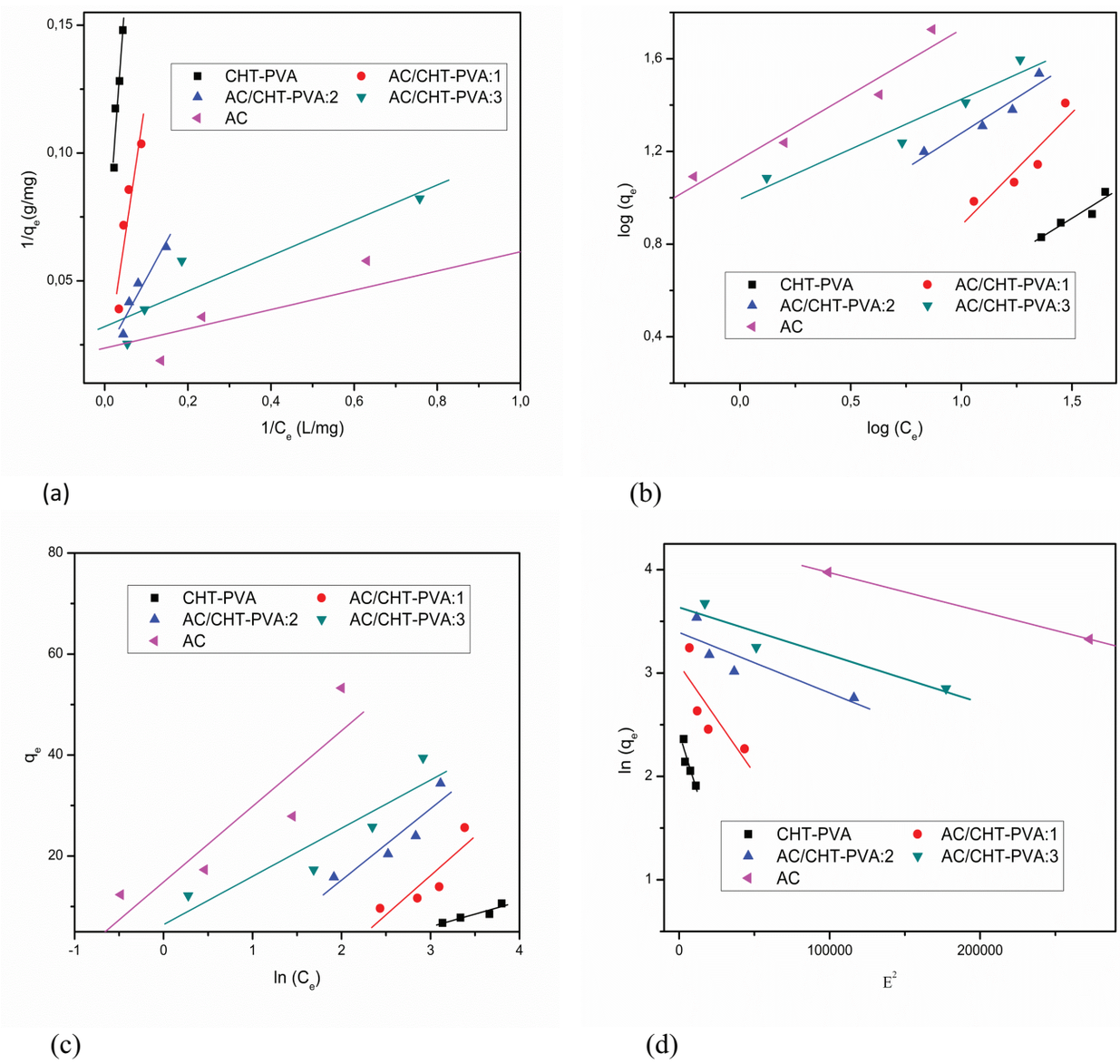

Fig. 9. Adsorption isotherms of the naproxen adsorption (a) Langmuir (b) Freundlich (c) Temkin (d) Dubinin-Radushkevich.

The plots of q_t against $t^{0.5}$ for intra-particle diffusion kinetic model are exhibited in Fig. 11c. k_{int} (mg/g·min$^{0.5}$) is rate constant. For intra-particle model, the straight line plots presenting two parts indicate two transport steps take place.

The plots of q_t versus ln$t$ for Elovich's model are demonstrated in Fig. 11d. According to the model, α is the adsorption rate (mg/g·min) constant and 1/β (mg/g) is number of available sites. Bangham kinetic model is displayed in Fig. 11e.

The calculated value of k_1, k_2, h, and q_e and R^2 values are demonstrated in Table 5. For pseudo first order model, despite the experimental q_e value ($q_{e,exp}$) was found as 12.256; q_e value calculated as 84.08 mg/g for AC/CHT-PVA:3.0. Although R^2 values were between 0.92 and 0.99, q_e values determined from the significantly different from experimental q_e values indicating the model is not suitable for describing the naproxen adsorption.

For the pseudo second-order kinetics model, the lines of (t/q_t) against t (min) presented in Fig. 11b. R^2 values were 0.99 for all biocomposites and experimental q_e values were nearly the same calculated ones (for AC/CHT-PVA:1.0 $q_{e,exp}$ = 9.6064 mg/g and $q_{e,cal}$ = 9.7371 mg/g; for AC/CHT-PVA:2.0 $q_{e,exp}$ = 11.372 mg/g and $q_{e,cal}$ = 11.5603 mg/g; for AC/CHT-PVA:3.0 $q_{e,exp}$ = 12.256 mg/g and $q_{e,cal}$ = 12.500 mg/g). h (adsorption rate constant) value was calculated as 1.7495 mg/g/min for AC; while biocomposites' adsorption rates were calculated as 1.1549 for AC/CHT-PVA:1.0; 1.5762 for AC/CHT-PVA:2.0; and 1.6767 for AC/CHT-PVA:3.0 (Table 5). These results implied that, the

Table 4
Kinetic models equations

Pseudo first order kinetic model	$\log(q_e - q_t) = \log(q_e) - (\frac{k_1}{2.303}) \cdot t$
Pseudo second order kinetic model	$\frac{t}{q_t} = \frac{1}{k_2 \cdot q_e^2} + \frac{1}{q_e} t$
Weber–Morris intra-particle diffusion kinetic model	$q_t = k_{id} t^{0.5} + C$
Elovich kinetic model	$q_t = \frac{1}{\beta} \ln(\alpha\beta) + \frac{1}{\beta} \ln(t)$
Bangham kinetic model	$\log\left[\log\left(\frac{C_0}{C_0 - q_t m}\right)\right] = \log\left(\frac{k_0 m}{2.303 V}\right) + \alpha \log(t)$

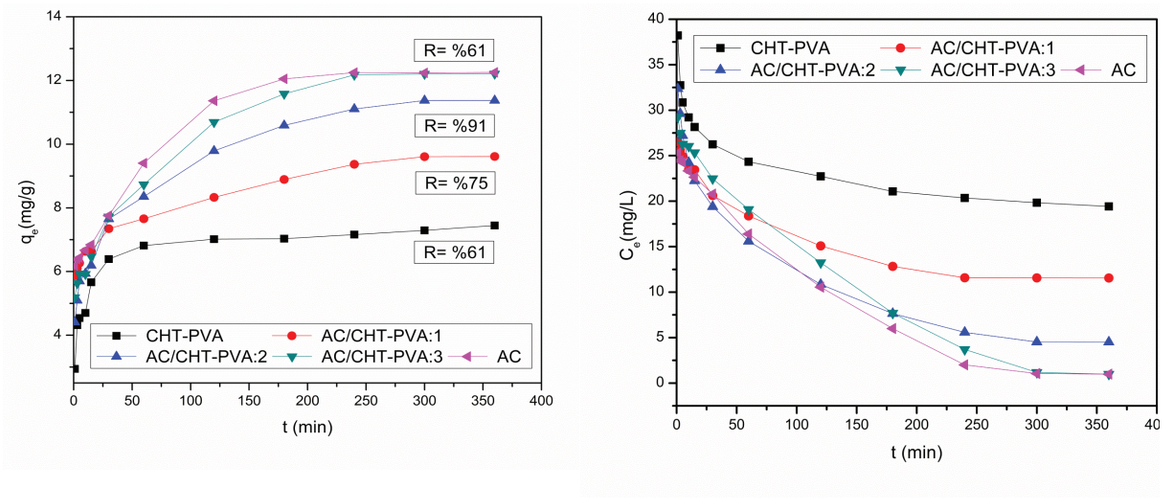

Fig. 10. Effect of time on the naproxen adsorption.

naproxen adsorption from factory wastewater onto all biocomposites represented better by the pseudo second-order kinetic model.

R^2 values for Weber–Morris intra-particle diffusion were calculated between (R^2 = 0.80–0.95) were lower than pseudo-second order kinetic model. From Fig. 11c and Table 2, two separate multi linear phase showed, which can be explain as different mass transfer phenomena occur. The first sharper linear part (phase I, first 7.5 min) attributed the boundary layer diffusion effect and mass transfer through the external surface of biocomposites. The second linear part (phase II) characterized the intra-particle diffusion effect and gradual mass transfer. According to Table 5, k_{id-1} and k_{id-2} constants for AC/CHT- PVA:3.0 (k_{id-1} = 0.3558 mg/g·min$^{0.5}$; k_{id-2} = 0.3965 mg/g·min$^{0.5}$), represented that, intra particle diffusion rate was faster than boundary layer mass transfer rate. Also, k_{id-1} and k_{id-2} constants for AC/CHT-PVA:1.0 and AC/CHT-PVA:2.0 were calculated as k_{id-1} = 0.3049 mg/g·min$^{0.5}$ and k_{id-2} = 0.1079 mg/g·min$^{0.5}$; k_{id-1} = 0.6100 mg/g·min$^{0.5}$ and; k_{id-2} = 0.2028 mg/g·min$^{0.5}$, respectively. These results described boundary layer mass transfer rate was three fold interior mass transfer.

Despite the correlation coefficients (R^2) for Elovich model were calculated between 0.86–0.98 and initial adsorption rate (α) values of all biocomposites decreased sharply with increasing activated carbon content (αAC/CHT-PVA:1.0 = 84.96 mg/g·min; αAC/CHT-PVA:3.0 = 49.69 mg/g·min). This result demonstrated that, Elovich's model did not fit sufficiently the naproxen adsorption.

The R^2 values were determined between 0.90 and 0.99 for Bangham model, so pore diffusion played an important role during the naproxen adsorption.

3.5. Thermodynamic approaches on naproxen adsorption from a factory wastewater

Fig. 12 illustrates the effect of temperature on the naproxen adsorption from factory wastewater. In order

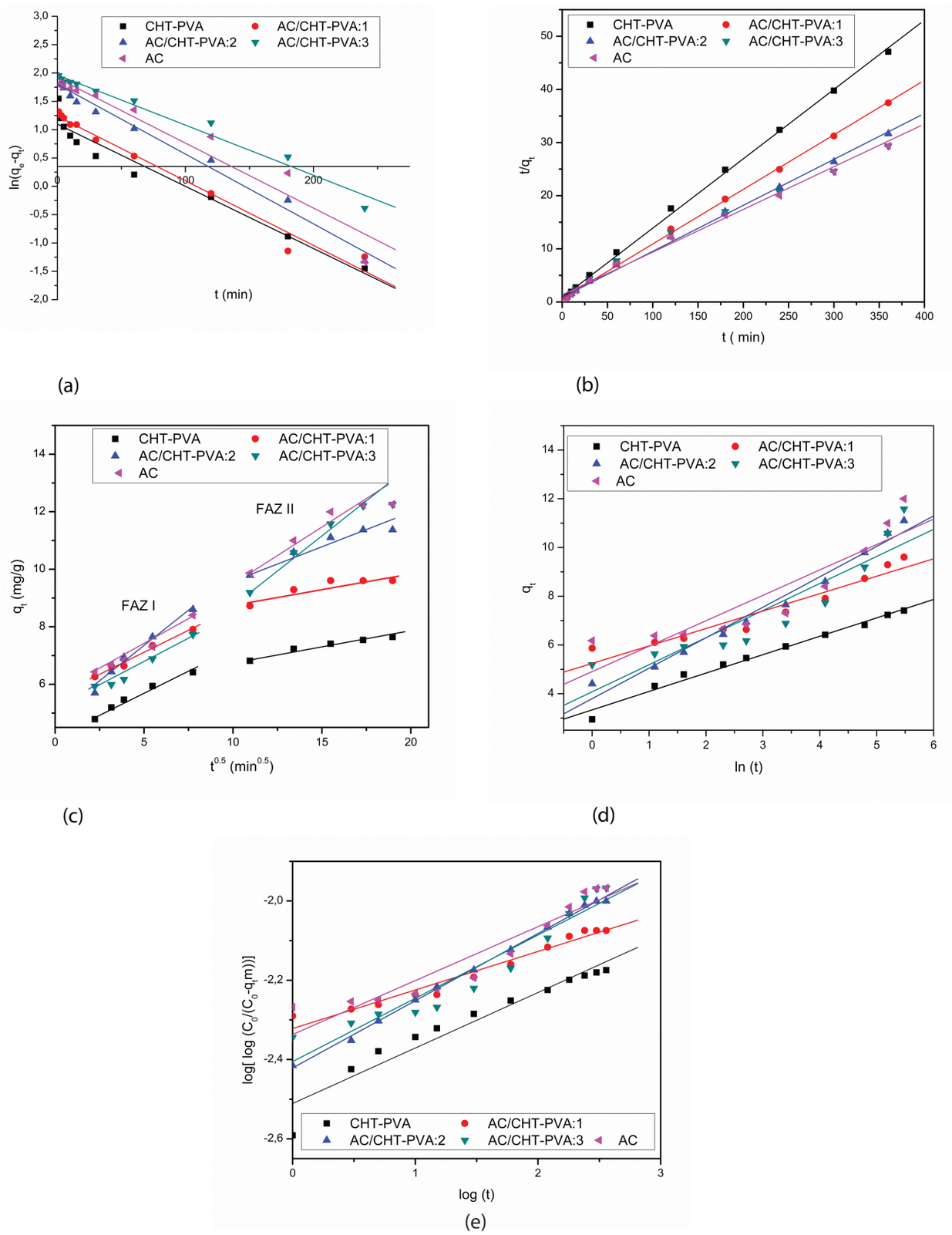

Fig. 11. Kinetic study of the naproxen adsorption (a) Pseudo-first order (b) Pseudo-second order (c) Weber–Morris intra-particle diffusion (d) Elovich (e) Bangham models.

Table 5
Adsorption kinetic model parameters of the naproxen adsorption

	CHT-PVA	AC/ CHT-PVA:1.0	AC/ CHT-PVA:2.0	AC/ CHT-PVA:3.0	AC
$q_{e,experimental}$ (mg/g)	7.6450	9.6064	11.372	12.256	12.263
Pseudo-first order kinetic model					
q_e (mg/g)	13.740	19.151	59.238	84.080	66.665
k_1 (min^{-1})	0.0264	0.0300	0.0260	0.0173	0.0196
R^2	0.92	0.99	0.98	0.99	0.99
Pseudo-second order kinetic model					
q_e (mg/g)	7.6628	9.7371	11.560	12.500	12.658
k^2(g/mg·min)	0.0202	0.0163	0.0118	0.0107	0.0109
h (mg/g·min)	1.1852	1.1549	1.5762	1.6767	1.7495
R^2	0.99	0.99	0.99	0.99	0.99
Weber–Morris intra-particle diffusion kinetic model					
$k_{id\text{-}1}$ (mg/g·$min^{0.5}$)	0.4411	0.3049	0.6100	0.3558	0.3194
R^2	0.8159	0.9891	0.9566	0.9802	0.9667
$k_{id\text{-}2}$ (mg/g·$min^{0.5}$)	0.1004	0.1079	0.2028	0.3965	0.3106
R^2	0.95	0.80	0.91	0.94	0.89
Elovich kinetic model					
β (g/mg)	1.3463	1.3548	0.7783	0.7738	0.8474
α (mg/g·min)	67.97	84.96	50.99	49.69	60.41
R^2	0.98	0.94	0.98	0.87	0.86
Bangham kinetic model					
k_0 (L/g)	1.76E–03	2.74E–03	3.46E–03	4.20E–03	5.68E–03
α	0.1001	0.0972	0.1295	0.1359	0.1596
R^2	0.93	0.96	0.99	0.90	0.92

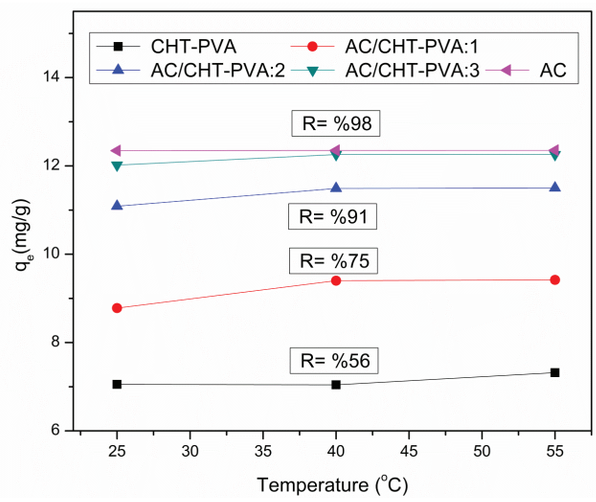

Fig. 12. Thermodynamic study of the naproxen adsorption.

to investigate the temperature effect, the adsorption of naproxen onto AC/CHT-PVA biocomposites were performed at 25°C, 40°C, and 55°C. Adsorption removal (%) values increased from 56% to 98% obviously with increasing activated carbon content but also, while temperature increased, q_e values were not changed significantly. It can be explained that, as the temperature raises, the energy content increases, so, the biocomposites requires more energy to remain in wastewater, thus directly affecting the adsorption balance.

Gibbs free energy change (ΔG°), enthalpy change (ΔH°) and entropy change (ΔS°), were determined and ΔH°, ΔG°, and ΔS° values for all biocomposites and activated carbon are exhibited in Table 6.

The standard Gibbs free energy values for the naproxen adsorption onto AC/CHT-PVA:3.0 was obtained as –7.979 kJ/mol, –10.192 kJ/mol and –10.709 kJ/mol at 25°C, 40°C, and 55°C, respectively. The negative ΔG^0 values indicated that adsorption is spontaneous process and negative values of ΔG° declined with raising temperature present spontaneous behavior of naproxen adsorption changed inversely with temperature. For all temperatures and biocomposites, the negative Gibbs free energy values showed that, AC/CHT-PVA biocomposites spontaneously adsorbed naproxen in solution. The positive entropy values point out an increasing of disorderliness and chaos at the solid/liquid interface and affinity of biocomposites towards naproxen. The endothermic behavior of the naproxen adsorption was proved by the positive values of ΔH^0 and also ΔH^0 value can be used to identify chemical or physical adsorption. For chemical adsorption, ΔH^0 is higher than 35 kJ/mol while for physical adsorption it is lower than 35 kJ/mol. It can be seen clearly from table that, the positive enthalpy values showed naproxen adsorption for all biocomposites were endother-

mic reaction so an increase of temperature promote the adsorption reaction. Also, low ΔH^0 values demonstrate evidence that, the synergy between naproxen and AC/CHT-PVA was not very strong. As a result, we concluded that naproxen adsorption by AC/CHT-PVA biocomposite is a physical adsorption process [31,32].

4. Conclusion

In the present work, activated carbon embedded chitosan-poly(vinyl alcohol) biocomposites were synthesized and applied for non steroidal anti-inflammatory drug naproxen adsorption from factory wastewater in Istanbul/Turkey. Naproxen removal performance increased from nearly 41% to 97% with an increasing AC content resulted in a large specific surface area according to BET analysis results. Also, our study showed that all AC/CHT-PVA biocomposites have a higher thermal stability compared to the CHT-PVA.The Langmuir model was fitted to the equilibrium data better than the other isotherm models and the kinetic of naproxen adsorption process is the best described by the pseudo second-order and Bangham models, so pore diffusion played an important role during the naproxen adsorption process. By evaluating the data of characterization of AC/CHT-PVA biocomposites and adsorption processes and values of kinetics parameters, enthalpy, entropy, and Gibbs free energy, it can be safely concluded that AC embedded CHT-PVA biocomposites have a potential as an adsorbent for the adsorption of non steroidal anti-inflammatory drug naproxen from factory wastewater.

References

[1] M. Carballa, F. Omil, J.M. Lema, M. Llompart, C. Garcia-Jares, I. Rodriguez, M. Gomez, Behavior of pharmaceuticals, cosmetics and hormones in a sewage treatment plant, Water Res., 38(12) (2004) 2918–2926.

[2] D.W. Kolpin, E.T. Furlong, M.T. Meyer, E.M. Thurman, S.D. Zaugg, L.D. Barber, H.T. Buxton, Pharmaceuticals, hormones, and other organic wastewater contaminants in US Streams, 1999–2000: A National reconnaissance, Environ. Sci. Technol., 36(6) (2002) 1202–1211.

[3] P.E. Stackelberg, E.T. Furlong, M.T. Meyer, S.D. Zaugg, A.K. Henderson, D.B. Reissman, Persistence of pharmaceutical compounds and other organic wastewater contaminants in a conventional drinking-water treatment plant, Sci. Total Environ., 329(1–3) (2004) 99–113.

[4] D. Barcelo, M. Petrovic, Pharmaceuticals and personal care products (PPCPs) in the environment, Anal. Bioanal. Chem., 387 (2007) 1141–1142.

[5] B. Subedi, B. Du, C.K. Chambliss, J. Koschorreck, H. Rudel, M. Quack, B.W. Brooks, S. Usenko, Occurrence of pharmaceuticals and personal care products in German fish tissue: A national study, Environ. Sci. Technol., 46 (2012) 9047–9054.

[6] K.K. Barnes, D.W. Kolpin, E.T. Furlong, S.D. Zaugg, M.T. Meyer, L.B. Barber, A National reconnaissance of pharmaceuticals and other organic wastewater contaminants in the United States - I) groundwater, Sci. Total Environ., 402 (2008) 192–200.

[7] M. Quire, M. Khamis, F. Malek, S. Nir, B. Abbadi, L. Scrano, Stability and removal of naproxen and its metabolite by advanced membrane wastewater treatment plant and micelle–clay complex, Clean- Soil Air Wat., 41 (2013) 1–7.

[8] C. Tixier, H.P. Singer, S. Oellers, S.R. Muller, Occurrence and fate of carbamazepine, clofibric acid, diclofenac, ibuprofen, ketoprofen, and naproxen in surface waters, Environ. Sci. Technol., 37 (2003) 1061–1068.

[9] G.R. Boyd, S. Zhang, D.A. Grimm, Naproxen removal from water by chlorination and biofilm processes, Water Res., 39 (2005) 668–676.

[10] P. Damiani, M. Bearzotti, M. Cabezan, Spectro fluorometric determination of naproxen in tablets, J. Pharm. Biomed. Anal., 29 (2002) 229–38.

[11] G. Boyd, S. Zhang, D. Grim, Naproxen removal from water by chlorination and biofilm processes, Water Res., 39 (2005) 668–676.

[12] G.R. Boyda, H. Reemtsmaa, D.S. Grimmb, S. Mitrac, Pharmaceuticals and personal care products (PPCPs) in surface and treated waters of Louisiana, USA and Ontario, Canada, Sci. Total Environ., 311 (2003) 135–49.

[13] H.E. Reynel-Avila, D.I. Medoza Costilla, A.B. Petriciolet, J.S. Albero, Assessment of naproxen adsorption on bone char in aqueous solutions using batch and fixed-bed processes, J. Mol. Liq., 209 (2015) 187–195.

[14] H.R. Busar, T. Poiger, M.D. Muller, Occurrence and fate of the pharmaceutical drug diclofenac in surface waters: rapid photo degradation in a lake, Environ. Sci. Technol., 32 (1998) 3449–556.

[15] A. Joss, S. Zabczynski, A. Gobel, B. Hoffmannc, D. Loffler, C.S. McArdell, T.A. Ternes, A. Thomsen, H. Siegrist, Biological degradation of pharmaceuticals in municipal wastewater treatment: proposing a classification scheme, Water Res., 4 (2006) 1686–1696.

[16] S. Esplugas, D.M. Bila, L. Gustavo, T. Krause, M. Dezotti, Ozonation and advanced oxidation technologies to remove endocrine disrupting chemicals (edcs) and pharmaceuticals and personal care products (Ppcps) in water effluents, J. Hazard. Mater., 149 (2007) 631–642.

[17] Z. Hasan, J. Jeon, S.H. Jhung, Adsorptive removal of naproxen and clofibric acid from water using metal–organic frameworks, J. Hazard. Mater., 209–210 (2012) 151–157.

[18] E.B. Simsek, D. Saloglu, N. Ozcan, I. Novak, D. Berek, Carbon fiber embedded chitosan/pva composites for decontamination of endocrine disruptor bisphenol-a from water, J. Taiwan Inst. Chem. Eng., 70 (2017) 291–301.

[19] J. Xu, L. Wang, Y. Zhu, Decontamination of bisphenol a from aqueous solution by graphene adsorption, Lang., 28 (2012) 8418–8425.

[20] G.A.F. Roberts, Chitin chemistry, the Macmillan Press Ltd, London, 1992.

[21] Y. Geng, M. Ding, H. Chen, H.F. Li, J.M. Lin, Preparation of hydrophilic carbon-functionalized magnetic micro spheres coated with chitosan and application in solid-phase extraction of bisphenol a in aqueous samples, Talanta, 89 (2012) 189–94 .

[22] V.E. Yudin, I.P. Dobrovolskaya, I.M. Neelova, E.N. Dresvyanina, P.V. Popryadukhin, E.M. Ivan'kova, Wet spinning of fibers made of chitosan and chitin nanofibrils, Carbohydr. Polym., 108 (2014)176–82 .

[23] D. Huang, W. Wang, J. Xu, A. Wang, Mechanical and water resistance properties of chitosan/poly (vinyl alcohol) films reinforced with attapulgite dispersed by high-pressure homogenization, Chem. Eng. J., 210 (2012)166–172 .

[24] D. Huang, B. Mu, A. Wang, Preparation and properties of chitosan/poly (vinyl alcohol) nano composite films reinforced with rod-like sepiolite, Mater. Lett., 86 (2012) 69–72 .

[25] H. Liao, R. Qi, M. Shen, X. Cao, R. Guo, Y. Zhang, X. Shi X, Improved cellular response on multi walled carbon nano tube-incorporated electro spun polyvinyl alcohol/chitosan nano fibrous scaffolds, Colloids Surf. B: Bio interfaces, 84 (2011) 528–535 .

[26] A.M. Pandele, M. Ionita, L. Crica, S. Dinescu, M. Costache, H. Iovu, Synthesis, characterization, and in-vitro studies of graphene oxide/chitosan–polyvinyl alcohol films, Carbohydr. Polym., 102 (2014) 813–820 .

[27] W.S.W. Ngah, L.C. Teong, M.A. Hanafiah, Adsorption of dyes and heavy metal ions by chitosan composites: a review, Carbohydr. Polym., 83 (2011) 1446–1456 .

[28] N.T. Nguyen, J.H. Liu, A green method for in situ synthesis of poly(vinyl alcohol)/chitosan hydrogel thin films with entrapped silver nano particles, J. Taiwan Inst. Chem. Eng., 45 (2014) 2827–2833 .

[29] D. Huang, W. Wang, Y. Kang, A. Wang, A chitosan/poly(vinyl alcohol) nano composite film reinforced with natural halloysite nanotubes, Polym. Comp., 33(10) (2012) 1693–1699 .
[30] C.S. Ozdemir, Y. Onal, Study to investigate the importance of mass transfer of naproxen sodium onto activated carbon, Chem. Eng. Process, 49 (2010) 1058–1065.
[31] A.O. Ifelebuegu, J.E. Ukpebor, C.C. Obidiegwu, B.C. Kwofi, L.E. Centre, comparative potential of black tea leaves waste to granular activated carbon in adsorption of endocrine disrupting compounds from aqueous solution, Global J. Environ. Sci. Manage, 1 (2015) 205–214.
[32] N. Isoda, R. Rodrigues, A. Silva, M. Gonçalves, D. Mandelli, F.C. Figueiredo, W.A. Carvalho, Optimization of preparation conditions of activated carbon from agriculture waste utilizing factorial design, Powder Technol., 256 (2014) 175–181.